J|A|C|S ARTICLES

Published on Web 12/30/2008

Self-Assembly of Dendritic Crowns into Chiral Supramolecular Spheres

Virgil Percec,*,† Mohammad R. Imam,†,‡ Mihai Peterca,‡ Daniela A. Wilson,† and Paul A. Heiney‡

Roy & Diana Vagelos Laboratories, Department of Chemistry, University of Pennsylvania, Philadelphia, Pennsylvania 19104-6323, and Department of Physics and Astronomy, University of Pennsylvania, Philadelphia, Pennsylvania 19104-6396

Received November 8, 2008; E-mail: percec@sas.upenn.edu

Abstract: The synthesis and structural and retrostructural analysis of a library of dendronized cyclotriveratrylene containing seven nonchiral and seven chiral self-assembling dendrons is reported. These dendronized cyclotriveratrylenes exhibit a crown conformation that we named dendritic crown. Selected examples of dendritic crowns self-assemble into helical pyramidal columns that self-organize into columnar crystals or into 2-D columnar hexagonal lattices with intracolumnar order. A second group of dendritic crowns self-assembles into helical pyramidal columns and spherical supramolecular dendrimers that self-organize into cubic and tetragonal lattices. A third group of dendritic crowns self-assembles only in spherical supramolecular dendrimers. The helical pyramidal columns and spherical supramolecular dendrimers assembled from dendronized cyclotriveratrylene containing nonchiral dendrons are chiral but racemic while those generated from chiral dendrons exhibit amplified chirality. Structural analysis by a combination of X-ray diffraction methods and CD experiments demonstrated a new mechanism for the assembly of chiral supramolecular spheres that involves an intramolecular structure containing short fragments of helical pyramidal columns.

Introduction

Dendrimers and dendrons[1] are monodisperse macromolecules with complex topologies that are synthesized by divergent[2] and convergent[3] iterative strategies. They are influential building blocks that impact science and technology at the interface between chemistry, biology, physics, medicine, and nanoscience.[4] Our laboratory discovered the first spherical supramolecular dendrimers that self-organize in a $Pm\bar{3}n$ cubic lattice.[5a] Rational design combined with structural and retrostructural analysis was used to establish that this periodic array is general for libraries of self-organizable spherical molecular and supramolecular dendrimers.[5] Spherical supramolecular dendrimers are self-assembled from conical or other conformers that represent a fragment of a sphere.[5a] They are generated from amphiphilic benzyl ether dendrons[5] and from a large variety of other self-assembling dendrons of similar shapes generated from more complex primary structures.[6] The mechanism of this self-assembly process was established by a combination of experiments that include X-ray diffraction (XRD),[5a] transmission electron microscopy (TEM),[7a,b] isomorphous replacement,[7c] advanced NMR methods,[7d] molecular simulations,[7e] and theoretical work.[7f,g] This mechanism facilitated the elaboration of design principles required for the construction of functional spherical supramolecular dendrimers,[8,9] and generated new

† Roy & Diana Vagelos Laboratories, Department of Chemistry, University of Pennsylvania.

‡ Department of Physics and Astronomy, University of Pennsylvania.

(1) (a) Fréchet, J. M. J.; Tomalia, D. A., Eds. *Dendrimers and Other Dendritic Polymers*; Wiley: New York, 2001. (b) Newkome, G. R.; Moorefield, C. N.; Vögtle, F. *Dendrimers and Dendrons*; Wiley-VCH: Weinheim, 2001.

(2) (a) Buhleier, E.; Wehner, W.; Vögtle, F. *Synthesis* **1978**, 155–158. (b) Tomalia, D. A.; Baker, H.; Dewald, J.; Hall, M.; Kallos, G.; Martin, S.; Roeck, J.; Ryder, J.; Smith, P. *Polymer J.* **1985**, *17*, 117–132. (c) Newkome, G. R.; Yao, Z.; Baker, G. R.; Gupta, V. K. *J. Org. Chem.* **1985**, *50*, 2003–2004.

(3) (a) Hawker, C. J.; Fréchet, J. M. J. *J. Am. Chem. Soc.* **1990**, *112*, 7638–7647. (b) Miller, T. M.; Neenan, T. X. *Chem. Mater.* **1990**, *2*, 346–349.

(4) (a) Moore, J. S. *Acc. Chem. Res.* **1997**, *30*, 402–413. (b) Kim, Y.; Zimmerman, S. C. *Curr. Opin. Chem. Biol.* **1998**, *2*, 733–742. (c) Seebach, D.; Rheiner, P. B.; Greiveldinger, G.; Butz, T.; Sellner, H. *Top. Curr. Chem.* **1998**, *197*, 125–164. (d) Majoral, J.-P.; Caminade, A.-M. *Top. Curr. Chem.* **1998**, *197*, 79–124. (e) Smith, D. K.; Diederich, F. *Chem. -Eur. J.* **1998**, *4*, 1353–1361. (f) Fischer, M.; Vögtle, F. *Angew. Chem., Int. Ed.* **1999**, *38*, 885–905. (g) Bosman, A. W.; Janssen, H. M.; Meijer, E. W. *Chem. Rev.* **1999**, *99*, 1665–1688. (h) Astruc, D.; Chardac, F. *Chem. Rev.* **2001**, *101*, 2991–3024. (i) Haag, R. *Chem. -Eur. J.* **2001**, *7*, 327–335. (j) Hecht, S.; Fréchet, J. M. J. *Angew. Chem., Int. Ed.* **2001**, *40*, 74–91. (k) Tully, D. C.; Fréchet, J. M. J. *Chem. Commun.* **2001**, 1229–1239. (l) Stiriba, S.-E.; Frey, H.; Haag, R. *Angew. Chem., Int. Ed.* **2002**, *41*, 1329–1334. (m) Esfand, R.; Tomalia, D. A. *Drug Discovery Today* **2001**, *6*, 427–436. (n) Gillies, E. R.; Fréchet, J. M. J. *Drug Discovery Today* **2005**, *10*, 35–43. (o) Jiang, D.-L.; Aida, T. *Polym. Prog. Sci.* **2005**, *30*, 403–422. (p) Van de Coevering, R.; Gebbink, R. J. M. K.; Van Koten, G. *Prog. Polym. Sci.* **2005**, *30*, 474–490. (q) Caminade, A.-M.; Majoral, J.-P. *Prog. Polym. Sci.* **2005**, *30*, 491–505. (r) Boas, U.; Heegaard, P. M. H. *Chem. Soc. Rev.* **2004**, *33*, 43–63. (s) Grinstaff, M. W. *Chem. -Eur. J.* **2002**, *8*, 2838–2846. (t) Grayson, S. M.; Fréchet, J. M. J. *Chem. Rev.* **2001**, *101*, 3819–3867. (u) Ponomarenko, S. A.; Boiko, N. I.; Shibaev, V. P. *Polym. Sci. Ser. C* **2001**, *43*, 1–45. (v) Suárez, M.; Lehn, J.-M.; Zimmerman, S. C.; Skoulios, A.; Heinrich, B. *J. Am. Chem. Soc.* **1998**, *120*, 9526–9532. (w) Diele, S. *Curr. Opin. Colloid Interface Sci.* **2002**, *7*, 333–342. (x) Baars, M. W. P. L.; Söntjens, S. H. M.; Fischer, H. M.; Peerlings, H. W. I.; Meijer, E. W. *Chem. -Eur. J.* **1998**, *4*, 2456–2466. (y) Matthews, O. A.; Shipway, A. N.; Stoddart, J. F. *Prog. Polym. Sci.* **1998**, *23*, 1–56.

 10.1021/ja8087778 CCC: $40.75

strategies to mediate functions.[9−12] Conical dendrons self-assemble also in $Im\bar{3}m$ cubic,[10a,b] $P4_2/mnm$ tetragonal,[10c] and 12-fold liquid quasicrystal semiperiodic arrays.[10d] Spherical supramolecular dendrimers were originally considered to consist of a disordered micellar structure.[5a] Recently, the first examples of hollow spherical supramolecular dendrimers assembled from conical dendrons that are chiral was reported.[11] They represent the first examples of spherical supramolecular dendrimers that exhibit internal helical order and therefore, are not micellar. Therefore, spherical supramolecular dendrimers with internal order are the most primitive synthetic mimics of globular proteins.[11]

The self-assembly of conical dendrons into spherical supramolecular dendrimers evolved from the assembly of tapered dendrons into columnar supramolecular dendrimers.[11−13] Many of the columnar dendrimers are helical and therefore are chiral.[12] The internal order of the columnar supramolecular dendrimers was analyzed by wide-angle XRD experiments performed on oriented fibers by transplanting methods from structural biology to supramolecular chemistry.[13] These experiments are facilitated by the anisotropic nature of the lattice self-organized from columnar supramolecular dendrimers. However, the cubic lattices self-organized from spherical supramolecular dendrimers are isotropic and therefore, wide-angle XRD experiments performed on their oriented fibers of monodomains do not provide information on their internal order.

(5) (a) Balagurusamy, V. S. K.; Ungar, G.; Percec, V.; Johansson, G. *J. Am. Chem. Soc.* **1997**, *119*, 1539–1555. (b) Percec, V.; Cho, W. D.; Mosier, P. E.; Ungar, G.; Yeardley, D. J. P. *J. Am. Chem. Soc.* **1998**, *120*, 11061–11070. (c) Ungar, G.; Percec, V.; Holerca, M. N.; Johansson, G.; Heck, J. A. *Chem. -Eur. J.* **2000**, *6*, 1258–1266. (d) Percec, V.; Cho, W. D.; Möller, M.; Prokhorova, S. A.; Ungar, G.; Yeardley, D. J. P. *J. Am. Chem. Soc.* **2000**, *122*, 4249–4250. (e) Percec, V.; Cho, W. D.; Ungar, G.; Yeardley, D. J. P. *Angew. Chem., Int. Ed. Engl.* **2000**, *39*, 1598–1602. (f) Percec, V.; Ahn, C. H.; Cho, W. D.; Jamieson, A. M.; Kim, J.; Leman, T.; Schmidt, M.; Gerle, M.; Möller, M.; Prokhorova, S. A.; Sheiko, S. S.; Cheng, S. Z. D.; Zhang, A.; Ungar, G.; Yeardley, D. J. P. *J. Am. Chem. Soc.* **1998**, *120*, 8619–8631. (g) Percec, V.; Cho, W. D.; Ungar, G. *J. Am. Chem. Soc.* **2000**, *122*, 10273–10281. (h) Percec, V.; Cho, W. D.; Ungar, G.; Yeardley, D. J. P. *J. Am. Chem. Soc.* **2001**, *123*, 1302–1315. (i) Cho, B.-K.; Jain, A.; Gruner, S. M.; Wiesner, U. *Science* **2004**, *305*, 1598–1601. (j) Bury, I.; Heinrich, B.; Bourgogne, C.; Guillon, D.; Donnio, B. *Chem. -Eur. J.* **2006**, *12*, 8396–8413. (k) Cho, B.-K.; Jain, A.; Mahajan, S.; Ow, H.; Gruner, S. M.; Wiesner, U. *J. Am. Chem. Soc.* **2004**, *126*, 4070–4071. (l) Frauenrath, H. *Prog. Polym. Sci.* **2005**, *30*, 325–384. (m) Coco, S.; Cordovilla, C.; Donnio, B.; Espinet, P.; Garcia-Casas, M. J.; Guillon, D. *Chem. -Eur. J.* **2008**, *14*, 3544–3552. (n) Saez, I. M.; Goodby, J. W.; Richardson, R. M. *Chem. -Eur. J.* **2001**, *7*, 2758–2764. (o) Chung, Y.-W.; Lee, J. K.; Zin, W.-C.; Cho, B.-K. *J. Am. Chem. Soc.* **2008**, *130*, 7139–7147. (p) Zeng, F.; Zimmerman, S. C. *Chem. Rev.* **1997**, *97*, 1681–1712. (q) Kim, H.-J.; Lee, E.; Kim, M. G.; Kim, M.-C.; Lee, M.; Sim, E. *Chem. -Eur. J.* **2008**, *14*, 3883–3888. (r) Ziherl, P.; Kamien, R. D. *Phys. Rev. Lett.* **2000**, *85*, 3528–3531. (s) Donnio, B; Buathong, S.; Bury, I.; Guillon, D. *Chem. Soc. Rev.* **2007**, *36*, 1495–1513. (t) Lenoble, J.; Campidelli, S.; Maringa, N.; Donnio, B.; Guillon, D.; Yevlampieva, N.; Deschenaux, R. *J. Am. Chem. Soc.* **2007**, *129*, 9941–9952. (u) Ungar, G.; Zeng, X. *Soft Matter* **2005**, *1*, 95–106. (v) Canilho, N.; Kasëmi, E.; Mezzenga, R.; Schlüter, A. D. *J. Am. Chem. Soc.* **2006**, *126*, 13998–13999. (w) Caminade, A.-M.; Turrin, C.-O.; Sutra, P.; Majoral, J.-P. *Curr. Opin. Colloid Interface Sci.* **2003**, *8*, 282–295. (x) Tschierske, C. *Curr. Opin. Colloid Interface Sci.* **2002**, *7*, 69–80.

(6) (a) Percec, V.; Mitchell, C. M.; Cho, W. D.; Uchida, S.; Glodde, M.; Ungar, G.; Zeng, X. B.; Liu, Y. S.; Balagurusamy, V. S. K.; Heiney, P. A. *J. Am. Chem. Soc.* **2004**, *126*, 6078–6094. (b) Percec, V.; Peterca, M.; Sienkowska, M. J.; Ilies, M. A.; Aqad, E.; Smidrkal, J.; Heiney, P. A. *J. Am. Chem. Soc.* **2006**, *128*, 3324–3334. (c) Percec, V.; Holerca, M. N.; Nummelin, S.; Morrison, J. L.; Glodde, M.; Smidrkal, J.; Peterca, M.; Rosen, B. M.; Uchida, S.; Balagurusamy, V. S. K.; Sienkowska, M. J.; Heiney, P. A. *Chem. -Eur. J.* **2006**, *12*, 6216–6241.

(7) (a) Hudson, S. D.; Jung, H. T.; Percec, V.; Cho, W. D.; Johansson, G.; Ungar, G.; Balagurusamy, V. S. K. *Science* **1997**, *278*, 449–452. (b) Hudson, S. D.; Jung, H. T.; Kewsuwan, P.; Percec, V.; Cho, W. D. *Liq. Cryst.* **1999**, *26*, 1493–1499. (c) Dukeson, D. R.; Ungar, G.; Balagurusamy, V. S. K.; Percec, V.; Johansson, G. A.; Glodde, M. *J. Am. Chem. Soc.* **2003**, *125*, 15974–15980. (d) Rapp, A.; Schnell, I.; Sebastiani, D.; Brown, S. P.; Percec, V.; Spiess, H. W. *J. Am. Chem. Soc.* **2003**, *125*, 13284–13297. (e) Li, Y. Y.; Lin, S. T.; Goddard III, W. A. *J. Am. Chem. Soc.* **2004**, *126*, 1872–1885. (f) Ziherl, P.; Kamien, R. D. *Phys. Rev. Lett.* **2000**, *85*, 3528–3531. (g) Ziherl, P.; Kamien, R. D. *J. Phys. Chem. B* **2001**, *105*, 10147–10158.

(8) (a) Percec, V.; Holerca, M. N.; Uchida, S.; Cho, W. D.; Ungar, G.; Lee, Y. S.; Yeardley, D. J. P. *Chem. -Eur. J.* **2002**, *8*, 1106–1117. (b) Percec, V.; Cho, W. D.; Ungar, G.; Yeardley, D. J. P. *Chem. -Eur. J.* **2002**, *8*, 2011–2025.

(9) (a) Percec, V.; Ahn, C. H.; Ungar, G.; Yeardley, D. J. P.; Möller, M.; Sheiko, S. S. *Nature* **1998**, *391*, 161–164. (b) Percec, V.; Ahn, C. H.; Barboiu, B. *J. Am. Chem. Soc.* **1997**, *119*, 12978–12979. (c) Percec, V.; Holerca, M. N. *Biomacromolecules* **2000**, *1*, 6–16. (d) Percec, V.; Holerca, M. N.; Magonov, S. N.; Yeardley, D. J. P.; Ungar, G.; Duan, H.; Hudson, S. D. *Biomacromolecules* **2001**, *2*, 706–728. (e) Percec, V.; Holerca, M. N.; Uchida, S.; Yeardley, D. J. P.; Ungar, G. *Biomacromolecules* **2001**, *2*, 729–740. (f) Felder, D.; Heinrich, B.; Guillon, D.; Nicoud, J.-F.; Nierengarten, J.-F. *Chem. -Eur. J.* **2000**, *6*, 3501–3507. (g) Nierengarten, J.-F.; Oswald, L.; Eckert, J.-F.; Nicoud, J.-F.; Armaroli, N. *Tetrahedron Lett.* **1999**, *40*, 5681–5684. (h) Eckert, J.-F.; Byrne, D.; Nicoud, J.-F.; Oswald, L.; Nierengarten, J.-F.; Numata, M.; Ikeda, A.; Shinkai, S.; Armaroli, N. *New J. Chem.* **2000**, *24*, 749–758. (i) Fernández, G.; Sánchez, L.; Pérez, E. M.; Martín, N. *J. Am. Chem. Soc.* **2008**, *130*, 10674–10683. (j) van Ameijde, J.; Liskamp, R. M. J. *Org. Biomol. Chem.* **2003**, *1*, 2661–2669. (k) Meyers, S. R.; Juhn, F. S.; Griset, A. P.; Luman, N. R.; Grinstaff, M. W. *J. Am. Chem. Soc.* **2008**, *130*, 14444–14445. (l) Giles, M. D.; Liu, S.; Emanuel, R. L.; Gibb, B. C.; Grayson, S. M. *J. Am. Chem. Soc.* **2008**, *130*, 14430–14431. (m) Fuchs, S.; Pla-Quintana, A.; Mazères, S.; Caminade, A.-M.; Majoral, J.-P. *Org. Lett.* **2008**, *10*, 4751–4754.

(10) (a) Yeardley, D. J. P.; Ungar, G.; Percec, V.; Holerca, M. N.; Johansson, G. *J. Am. Chem. Soc.* **2000**, *122*, 1684–1689. (b) Duan, H.; Hudson, S. D.; Ungar, G.; Holerca, M. N.; Percec, V. *Chem. -Eur. J.* **2001**, *7*, 4134–4141. (c) Ungar, G.; Liu, Y. S.; Zeng, X. B.; Percec, V.; Cho, W. D. *Science* **2003**, *299*, 1208–1211. (d) Zeng, X. B.; Ungar, G.; Liu, Y. S.; Percec, V.; Dulcey, A. E.; Hobbs, J. K. *Nature* **2004**, *428*, 157–160.

(11) Percec, V.; Peterca, M.; Dulcey, A. E.; Imam, M. R.; Hudson, S. D.; Nummelin, S.; Adelman, P.; Heiney, P. A. *J. Am. Chem. Soc.* **2008**, *130*, 13079–13094.

(12) (a) Percec, V.; Dulcey, A. E.; Balagurusamy, V. S. K.; Miura, Y.; Smidrkal, J.; Peterca, M.; Nummelin, S.; Edlund, U.; Hudson, S. D.; Heiney, P. A.; Hu, D. A.; Magonov, S. N.; Vinogradov, S. A. *Nature* **2004**, *430*, 764–768. (b) Percec, V.; Dulcey, A. E.; Peterca, M.; Ilies, M.; Miura, Y.; Edlund, U.; Heiney, P. A. *Aust. J. Chem.* **2005**, *58*, 472–482. (c) Percec, V.; Dulcey, A. E.; Peterca, M.; Ilies, M.; Ladislaw, J.; Rosen, B. M.; Edlund, U.; Heiney, P. A. *Angew. Chem., Int. Ed.* **2005**, *44*, 6516–6521. (d) Percec, V.; Dulcey, A. E.; Peterca, M.; Ilies, M.; Sienkowska, M. J.; Heiney, P. A. *J. Am. Chem. Soc.* **2005**, *127*, 17902–17909. (e) Percec, V.; Dulcey, A. E.; Peterca, M.; Ilies, M.; Nummelin, S.; Sienkowska, M. J.; Heiney, P. A. *Proc. Natl. Acad. Sci. U. S. A.* **2006**, *103*, 2518–2523. (f) Peterca, M.; Percec, V.; Dulcey, A. E.; Nummelin, S.; Korey, S.; Ilies, M.; Heiney, P. A. *J. Am. Chem. Soc.* **2006**, *128*, 6713–6720. (g) Percec, V.; Dulcey, A. E.; Peterca, M.; Adelman, P.; Samant, R.; Balagurusamy, V. S. K.; Heiney, P. A. *J. Am. Chem. Soc.* **2007**, *129*, 5992–6002. (h) Percec, V.; Rudick, J. G.; Peterca, M.; Wagner, M.; Obata, M.; Mitchell, C. M.; Cho, W. D.; Balagurusamy, V. S. K.; Heiney, P. A. *J. Am. Chem. Soc.* **2005**, *127*, 15257–15264. (i) Percec, V.; Smidrkal, J.; Peterca, M.; Mitchell, C. M.; Nummelin, S.; Dulcey, A. E.; Sienkowska, M. J.; Heiney, P. A. *Chem. -Eur. J.* **2007**, *13*, 3989–4007. (j) Kaucher, M. S.; Peterca, M.; Dulcey, A. E.; Kim, A. J.; Vinogradov, S. A.; Hammer, D. A.; Heiney, P. A.; Percec, V. *J. Am. Chem. Soc.* **2007**, *129*, 11698–11699. (k) Percec, V.; Won, B.; Peterca, M.; Heiney, P. A. *J. Am. Chem. Soc.* **2007**, *129*, 11265–11278. (l) Rudick, J. G.; Percec, V. *Acc. Chem. Res.* **2008**, *41*, 1641–1652. (m) Percec, V. *Philos. Trans. R. Soc. A.* **2006**, *364*, 2709–2719. (n) Percec, V.; Rudick, J. G.; Peterca, M.; Heiney, P. A. *J. Am. Chem. Soc.* **2008**, *130*, 7503–7508. (o) Rudick, J. G.; Percec, V. *Macromol. Chem. Phys.* **2008**, *209*, 1759–1768. (p) Rudick, J. G.; Percec, V. *New J. Chem.* **2007**, *31*, 1083–1096.

(13) Peterca, M.; Percec, V.; Imam, M. R.; Leowanawat, P.; Morimitsu, K.; Heiney, P. A. *J. Am. Chem. Soc.* **2008**, *130*, 14840–14852.

Scheme 1. Dendronized Cyclotriveratrylene (**CTV**) Derivatives

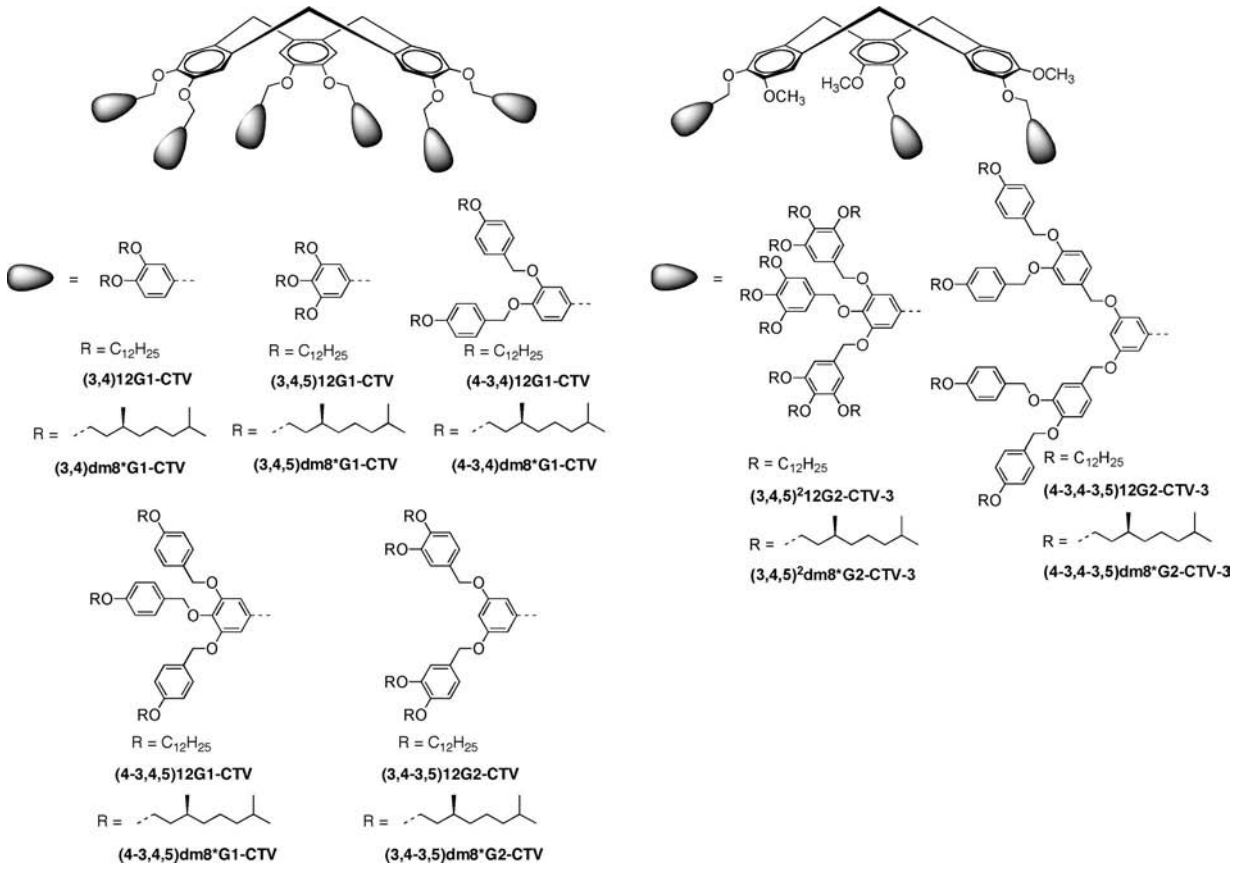

A recent publication from our laboratory determined the molecular structure and the mechanisms for the formation of helical dendrimers from supramolecular columns.[13] One of the discoveries reported in this work[13] showed that the dendritic crown, a conformation that can be hollow or nonhollow, molecular or supramolecular, provides the most general mechanism for the assembly of helical supramolecular dendrimers. This discovery was facilitated by the relatively rigid cyclotriveratrylene (CTV) crown that was used as a model.[13,14] CTV containing alkyl side groups exhibits a crown conformation that self-assemble into pyramidal columns.[14,15] Some of these pyramidal columns were shown to be helical.[14,15] Dendronized CTV generate dendritic crowns that self-assemble into helical pyramidal columns.[13]

This work reports that dendronized CTV form dendritic crowns that self-assemble also into spherical supramolecular dendrimers that are chiral. These chiral supramolecular dendrimers self-organize in $Pm\bar{3}n$ cubic and $P4_2/mnm$ tetragonal lattices. The self-assembly of dendritic crowns into chiral supramolecular spheres represents a new self-assembly mechanism that may open unprecedented scientific and practical opportunities.

Results and Discussion

Dendronized Cyclotriveratrylenes as Models for Crown-Like Dendrons and Dendrimers that Self-Assemble into Spherical Supramolecular Dendrimers. Scheme 1 outlines the structures of the library of dendronized CTV that will be discussed in this report. The synthesis and the analytical data of these dendronized CTV are presented in the Supporting Information. This library contains seven nonchiral and seven chiral dendronized CTV. Table 1 summarizes the phase transitions of the supramolecular structures assembled from the dendronized CTV shown in Scheme 1. These results were generated by a combination of Differential Scanning Calorimetry (DSC) and XRD experiments.[5a] (3,4)12G1-CTV, (3,4)dm8*G1-CTV, (4−3,4)12G1-CTV, (4−3,4)dm8*G1-CTV, (4−3,4−3,5)12G2-CTV-3, and (4−3,4−3,5)dm8*G2-CTV-3 self-assemble into pyramidal columns that self-organize in a hexagonal columnar lattice without (Φ_h) and with intracolumnar helical order (Φ_h^{io}). (3,4,5)12G1-CTV, (4−3,4,5)12G1-CTV, and (3,4−3,5)12G2-CTV self-assemble into pyramidal columns without (Φ_h) and with intracolumnar order (Φ_h^{io}) as well as in supramolecular spheres that self-organize in $Pm\bar{3}n$ cubic lattices. The replacement of the *n*-alkyl groups from the periphery of these dendronized CTV with a chiral alkyl group generates (3,4,5)dm8*G1-CTV, (4−3,4,5)dm8*G1-CTV, and (3,4−3,5)dm8*G2-CTV (Scheme 1). The chiral dendronized CTV eliminate the self-assembly in the pyramidal columns and self-assemble only in supramolecular spheres that self-organize in the $Pm\bar{3}n$ cubic

(14) (a) Collet, A. In *Comprehensive Supramolecular Chemistry*; Atwood, J. L., Davies, J. E. D., MacNicol, D. D., Vögtle, F., Eds.; Pergamon: New York, 1996; Vol. 6, pp. 281−303. (b) Collet, A. *Tetrahedron* **1987**, *43*, 5725–5759. (c) Malthête, J.; Collet, A *Nouv. J. Chim.* **1985**, *9*, 151–153. (d) Zimmermann, H; Poupko, R.; Luz, Z.; Billard, J. *Z. Naturforsch.* **1985**, *40a*, 149–160. (e) Malthête, J.; Collet, A. *J. Am. Chem. Soc.* **1987**, *109*, 7544–7545. (f) Poupko, R.; Luz, Z.; Spielberg, N.; Zimmermann, H. *J. Am. Chem. Soc.* **1989**, *111*, 6094–6105. (g) Lesot, P.; Merlet, D.; Sarfati, M.; Courtieu, J.; Zimmermann, H.; Luz, Z. *J. Am. Chem. Soc.* **2002**, *124*, 10071–10082. (h) Zimmermann, H.; Bader, V.; Poupko, R.; Wachtel, E. J.; Luz, Z. *J. Am. Chem. Soc.* **2002**, *124*, 15286–15301.

(15) Levelut, A. M.; Malthête, J.; Collet, A. *J. Phys. (Paris)* **1986**, *47*, 351–357.

Table 1. Thermal Analysis of the Supramolecular Dendrimers Self-Assembled from Dendronized CTV

dendrimer	phase transition [°C] and corresponding enthalpy changes [kcal mol^{-1}][a]	
	heating	cooling
(3,4)12G1-CTV	Φ_h^{io} 62.3 (7.34) Φ_h 154.1 (9.22) *i* Φ_h^{io} 63.6 (6.51) Φ_h 154.0 (9.20) *i*	*i* 146.8 (−7.75) Φ_h 61.8 (−6.66) Φ_h^{io}
(3,4)dm8*G1-CTV	*k* 48.2 (2.02) Φ_h^{io} 68.8 (13.30) Φ_h 76.2 (0.87) *i* Φ_h^{io} 67.8 (18.05) Φ_h 75.1 (0.61) *i*	*i* 57.8 (−21.81) Φ_h^{io}
(3,4,5)12G1-CTV	Φ_h^{io} 17.3 (3.87) Φ_h 69.2 (18.65) Cub 93.1 (0.67) *i* Φ_h^{io} −13.1 (11.12) Cub 51.7 (−4.57) Φ_h 68.6 (17.27) Cub 93.5 (0.80) *i*	*i* 75.8 (−0.38) Cub 59.5 (−0.67) Cub −16.4 (−10.67) Φ_h^{io}
(3,4,5)dm8*G1-CTV	T_g 2.3 Cub 45[b] *i* T_g −0.5 Cub 45[b] *i*	Cub 3.2 T_g
(4−3,4)12G1-CTV	Φ_h^{io} 82.9 (2.59) Φ_h 223.8 (19.65) *i* Φ_h 217.2 (6.68) *i*	*i* 209.0 (−7.79) Φ_h 84.6 (−1.85) $\Phi_{r\text{-}s}$
(4−3,4)dm8*G1-CTV	Φ_h^{io} 177.6 (6.24) Φ_h 233.2 (17.85) *i* Φ_h^{io} 174.7 (3.93) Φ_h 226.2 (8.69) *i*	*i* 217.6 (−9.73) Φ_h 166.6 (−3.20) Φ_h^{io}
(4−3,4,5)12G1-CTV	$\Phi_h^{crystal}$ 84.6 (3.37) Φ_h^{io} 104.9 (7.04) Cub 186.8 (1.04) *i* Cub_g −16.5 (14.85) Cub 82.8 (1.86) Cub 183.0 (0.65) *i*	*i* 165.9 (−0.48) Cub 71.8 (−1.29) Cub −22.3 (−10.42) Cub_g
(4−3,4,5)dm8*G1-CTV	T_g 75.1 Cub 143.8 (0.28) *i* T_g 65.9 Cub 143[b] *i*	Cub 55.2 T_g
(3,4−3,5)12G2-CTV	*k* −2.5 (13.32) Φ_h^{io} 67.3 (5.51) Cub 129.9 (1.71) *i* *k* −3.4 (16.32) Φ_h^{io} 69.5 (2.96) Cub 129.9 (1.70) *i*	*i* 118.2 (−0.67) Cub 68.6 (−4.12) Φ_h^{io} −8.0 (−13.19) *k*
(3,4−3,5)dm8*G2-CTV	T_g 41.1 Cub_g 70.0 (−0.19) Cub 89.0 (0.74) *i* Cub_g 67.6 (−0.28) Cub 89.0 (0.73) *i*	Cub 14.4 T_g
(4−3,4−3,5)12G2-CTV-3	$\Phi_h^{crystal}$ 126.8 (−7.00) Φ_h^{io} 168.1 (33.87) *i* $\Phi_h^{crystal}$ 39.1 (4.59) Φ_h^{io} 167.4 (33.73) *i*	*i* 143.5 (−30.64) Φ_h^{io} 30.0 (−6.58) $\Phi_h^{crystal}$
(4−3,4−3,5)dm8*G2-CTV-3	Φ_h^{io} 167.3 (35.60) *i* Φ_h^{io} 166.8 (6.01) *i*	*i* 137.8 (−33.68) Φ_h^{io}
$(3,4,5)^2$12G2-CTV-3	*k* −7.2 (24.33) Tet 100.6 (1.02) *i* *k* −6.8 (23.45) Tet 100.6 (1.02) *i*	*i* 81.9 (−0.25) Tet −11.2 (−21.38) *k*
$(3,4,5)^2$dm8*G2-CTV-3	T_g 24.7 *Tet* 80[b] *i* T_g 12.8 *Tet* 80[b] *i*	Tet_g

[a] Data from the first heating and cooling scans are on the first line, and data from the second heating are on the second line; *k* crystalline, Φ_h^{io}: columnar hexagonal lattice with intracolumnar order, $\Phi_h^{crystal}$: columnar hexagonal crystal, $\Phi_{r\text{-}s}$: *p2 mm* simple rectangular columnar LC phase, Φ_h: *p6 mm* hexagonal columnar LC phase, Cub: *Pm*$\bar{3}$*n* cubic lattice, Cub_g: glassy cubic phase, Tet: $P4_2/mnm$ tetragonal lattice, Tet_g: glassy tetragonal phase, T_g: glass transition, i: isotropic. [b] Phase observed only by TOPM and XRD.

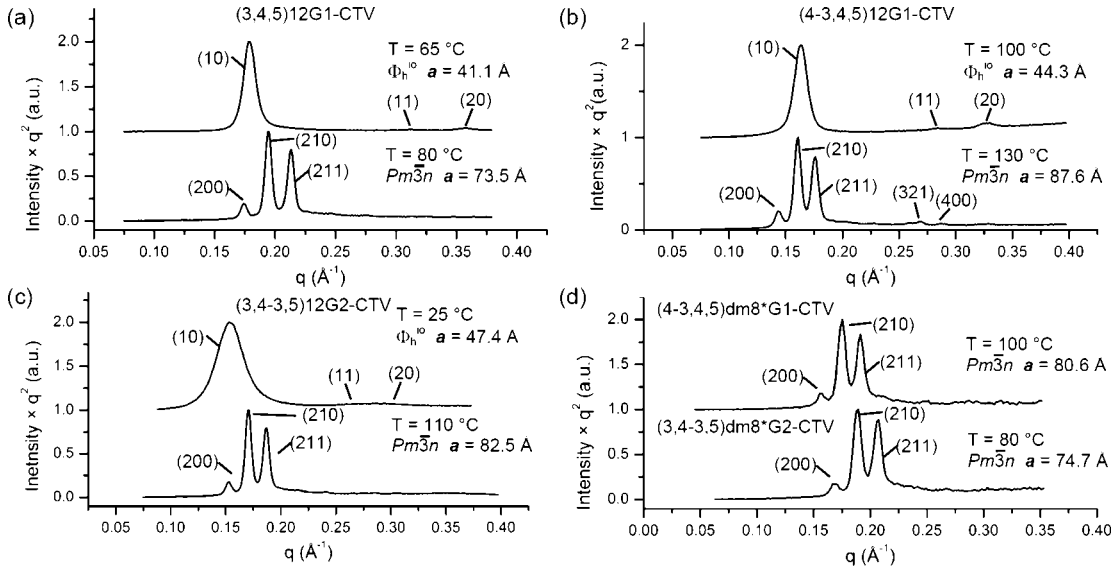

Figure 1. X-ray powder diffraction plots collected on dendronized CTV at the indicated temperatures. Phases, diffraction peaks indexing, and lattice dimensions are marked.

lattices (Table 1). Both $(3,4,5)^2$12G2-CTV-3 and $(3,4,5)^2$dm8*G2-CTV-3 self-assemble in supramolecular spheres that self-organize only in a tetragonal lattice.[10c]

Structural and Retrostructural Analysis of Helical Pyramidal and Spherical Supramolecular Dendrimers Self-Assembled from (4−3,4,5)12G1-CTV. We will discuss first the self-assembly of (4−3,4,5)12G1-CTV from Scheme 1. Figure 1 shows representative powder small-angle XRD plots obtained from the Φ_h^{io} and *Pm*$\bar{3}$*n* lattices self-assembled from (4−3,4,5)12G1-CTV and other dendronized CTV. The temperature, the indexing of the diffraction peaks and the lattice dimensions in each phase are indicated in Figure 1.

At room temperature (4−3,4,5)12G1-CTVs self-assemble into a columnar hexagonal crystal generated from helical pyramidal columns (Table 1). This structure is not yet completely elucidated. The fiber XRD of (4−3,4,5)12G1-CTV indicates in the crystal phase a helical pyramidal column (Figure 2). At 84.5 °C, this 3-D lattice transforms into helical pyramidal columns

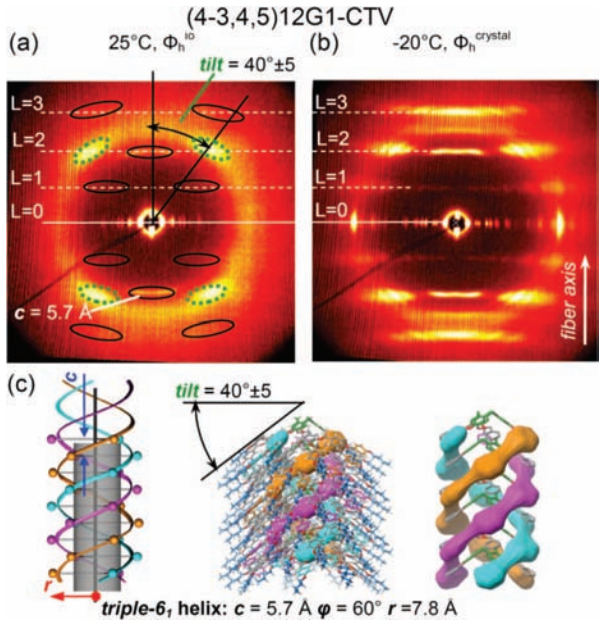

Figure 2. Wide angle X-ray diffraction patterns collected from the oriented fibers of the helical columnar Φ_h^{io} (a) and $\Phi_h^{crystal}$ (b) assemblies of (4−3,4,5)12G1-CTV at the indicated temperatures. Corresponding atomic and molecular helical models that fit the identified helical packing (c). The helical layer line features, tilt features, helix type, and triple-6_1 helix parameters are indicated.

self-organized in a Φ_h^{io} periodic array. The structure of the helical pyramidal column assembled in the Φ_h^{io} phase was previously analyzed[13] by the application of helical diffraction theory[16] to the atomic helix and by the Cerius2 simulation of its fiber XRD with a helical molecular model. The atomic structure of the helix in the crystal state was determined by helical diffraction theory (Figure 2) and is identical to that exhibited in the Φ_h^{io} phase.[13] At 104.9 °C, the Φ_h^{io} phase transforms in a $Pm\bar{3}n$ cubic lattice, that is assembled from supramolecular spheres. The upper left side of Figure 3 illustrates the well-established mechanism of self-assembly of tapered dendrons in helical columns followed by self-organization of the supramolecular column in a Φ_h or Φ_h^{io} lattice. The right side shows the assembly of a conical dendron in a spherical supramolecular dendrimer and its self-organization in a $Pm\bar{3}n$ cubic lattice.

The transition from a tapered to a conical dendron conformation and from the Φ_h or Φ_h^{io} lattice to a $Pm\bar{3}n$ cubic lattice is mediated by temperature.[5h] Under these conditions, the mechanism outlined in the upper part of Figure 3 must provide the lattice dimension of the Φ_h lattice (a_{hex}) equal to half of the lattice dimension of the $Pm\bar{3}n$ cubic lattice (a_{cub}), $a_{hex} \approx a_{cub}/2$. The lower part of the Figure 3 shows the electron density maps constructed from the XRD data from Figure 1b for the case of the Φ_h^{io} and $Pm\bar{3}n$ cubic lattices of (4−3,4,5)12G1-CTV. The lattice dimensions of the Φ_h^{io} phase and of the $Pm\bar{3}n$ cubic phase show the $a_{hex} \approx a_{cub}/2$ dependence. Therefore, on the basis of this dependence we can assume that the self-assembly mechanism maintains the overall organization within the supramolecular columns and spheres upon the phase transitions. Therefore, if a crown-like conformation was responsible for the assembly of the supramolecular column, the same crown conformation must be maintained during the transition to the supramolecular sphere. Under these conditions, the dendritic crown (4−3,4,5)12G1-CTV would not act as a conical conformer during the self-assembly in the supramolecular sphere as used to be the case in the previous self-assembly process.[5a] Figure 4 outlines the possible self-assembly of eight dendritic crowns derived from (4−3,4,5)12G1-CTV (Table 2) acting as conical conformers during the assembly of the spherical supramolecular dendrimer. The diameter of the theoretical sphere generated by this mechanism is $D_{sphere}^{th} = 69$ Å while the experimental value obtained from XRD is $D_{sphere}^{exp} = 54$ Å (Table 2). This disagreement between the much higher $D_{sphere}^{th} = 69$ Å and $D_{sphere}^{exp} = 54$ Å increases even more if the diameter of the sphere is calculated as the close contact direction between the centers of the two spheres from the face of the $Pm\bar{3}n$ lattice (Figure 3 and 5). The lack of agreement between the D_{sphere}^{th} and D_{sphere}^{exp} suggests that an alternative mechanism must be responsible for the self-assembly of dendritic crowns into the spherical supramolecular dendrimers.

Helical columns assembled from tapered dendrons or from dendritic crowns have a similar diameter. The molecular model of the triple-6_1 helical pyramidal column[13] assembled from (4−3,4,5)12G1-CTV in the Φ_h^{io} is shown in the bottom of Figure 5a and schematically in Figure 5b. The electron density map of the Φ_h^{io} lattice is in the left side of Figure 5a while that of $Pm\bar{3}n$ cubic lattice in the right side of the same figure. The $D_{column}^{exp} = a_{hex} = a_{cub}/2 = 44$ Å (Figure 5, Table 2). This result suggests that most probably the mechanism by which the supramolecular sphere is self-assembled from dendritic crowns is via the splitting of the helical pyramidal column into shorter fragments of column that adopt a spherical shape. This mechanism is outlined in Figure 5b. Three pathways are possible in this case. In the first model (left side of Figure 5b), the helical pyramidal column splits into shorter columns without the inversion of the conformation of the CTV crown. In the second model (middle of Figure 5b), inversion of conformation of the CTV crown produces two spheres with different polarity. The third model exhibits inversion of conformation of the CTV crown inside the sphere. Regardless of the mechanism responsible for this transition, the supramolecular spheres generated from fragments of helical pyramidal columns must be chiral. Experiments demonstrating this hypothesis will be presented in a different subchapter.

Structural Analysis of Helical Pyramidal Columns and Spherical Supramolecular Columns Assembled from Other Non-Chiral Dendritic Crowns. Two additional examples of dendronized CTV containing six nonchiral dendrons attached to CTV, (3,4,5)12G1-CTV and (3,4−3,5)12G2-CTV, were analyzed by DSC and XRD experiments (Tables 1 and 2, Figure 1). In both cases, experimental results suggest the same mechanism of assembly of the supramolecular sphere as in the case of (4−3,4,5)12G1-CTV. Experimental results of the self-assembly process for (3,4,5)12G1-CTV and (3,4−3,5)12G2-CTV are summarized in Table 2.

Two examples of dendronized CTV containing only three nonchiral dendrons attached to CTV were also analyzed by a combination of DSC and XRD experiments. (4−3,4−3,5)12G2-CTV-3 (Scheme 1, Table 3) self-assemble into a helical pyramidal column. The analysis of this helical pyramidal column by helical diffraction theory[13,16] applied to oriented fibers by wide-angle XRD demonstrated a triple-6_1 helix with the helical parameters summarized in Figure 6b,e. The molecular model of the helical pyramidal column generated by Cerius2 simulation

(16) (a) Cochran, W.; Crick, F. H. C.; Vand, V. *Acta Crystallogr.* **1952**, *5*, 581–586. (b) Klug, A.; Crick, F. H. C.; Wyckoff, H. W. *Acta Crystallogr.* **1958**, *11*, 199–213.

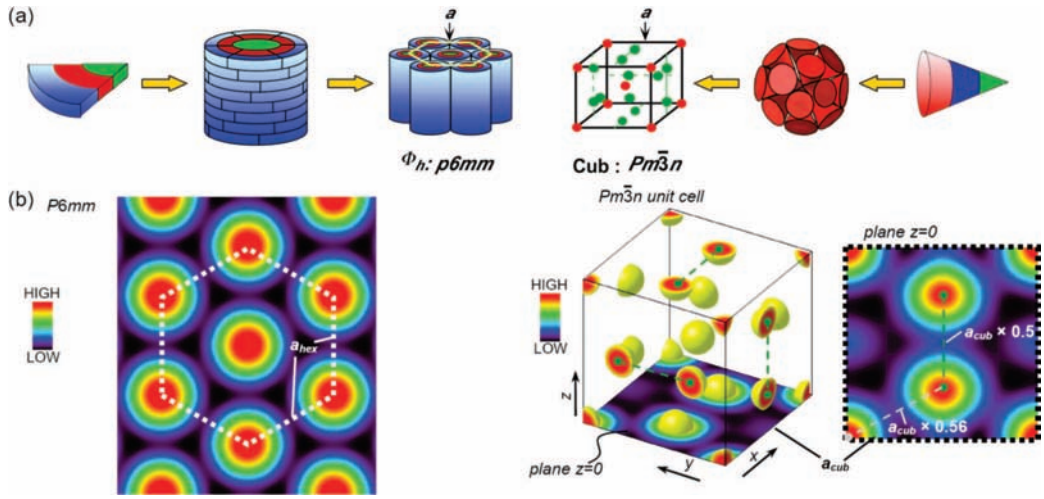

Figure 3. Schematic of the self-assembly process of taper and conical shaped dendrons into *p6mm* columnar hexagonal or *Pm*$\bar{3}$*n* cubic lattices (a) and the corresponding relative electron density distributions (b).

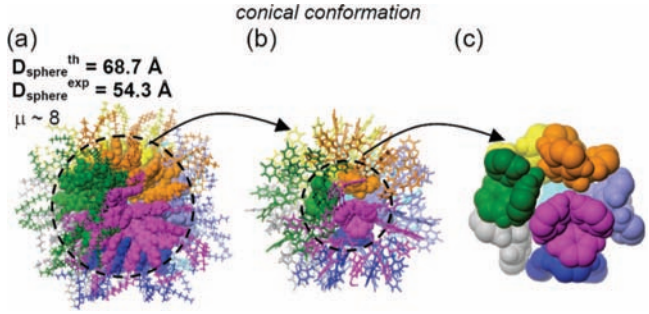

Figure 4. The molecular model of the self-assembly of the (4−3,4,5)12G1-CTV by conical conformer model.[5a] (a) Supramolecular sphere with the aromatic region shown in space filling view and the aliphatic region in stick view. (b) Detail of the aromatic region shown in stick view and the CTV core region in space filling view. (c) CTV core region shown in space filling view. Color code: In all cases, each of the eight dendrimers is colored differently.

is shown in Figure 6, parts c and f. $(3,4,5)^2$12G2-CTV-3 (Scheme 1, Table 3) self-assemble in supramolecular spheres that self-organize in a $P4_2/mnm$ tetragonal phase. The number of dendritic crowns per supramolecular sphere calculated for this phase is $\mu = 5$ (Table 3) and the assembly model is illustrated in Figure 7. The crown conformer model of the helical sphere from Figure 7 indicates that the mechanism from the right column of Figure 5b is the most feasible for the assembly of a helical sphere from dendritic crowns.

Structural Analysis of Chiral Dendronized CTV by XRD. The *Pm*$\bar{3}$*n* cubic phase and $P4_2/mnm$ tetragonal phase are isotropic, and oriented fibers or monodomains cannot be used for the analysis of the intramolecular structure of the supramolecular sphere by a combination of small- and wide-angle experiments. Therefore, in order to provide support for the helical chiral structure generated from helical supramolecular spheres, we have synthesized all nonchiral dendronized CTV in their chiral form. The structures of all chiral compounds are summarized in Scheme 1. The stereocenter was incorporated in all cases in the alkyl group of the dendron. The following five new chiral dendronized CTV were synthesized for the first time: (3,4,5)dm8*G1-CTV, (4−3,4,5)dm8*G1-CTV, (3,4−3,5)dm8*G2-CTV, (4−3,4−3,5)dm8*G2-CTV-3 and $(3,4,5)^2$dm8*G2-CTV-3 (Scheme 1). Their synthesis and analytical data are reported in the Supporting Information. (3,4)dm8*G1-CTV and (4−3,4)-dm8*G1-CTV from Scheme 1 were previously reported.[13]

The thermal transitions determined by a combination of DSC and XRD are summarized in Table 1. It is interesting to observe that the transition from (3,4)12G1-CTV to (3,4)dm8*G1-CTV, from (4−3,4)12G1-CTV to (4−3,4)dm8*G1-CTV, and from $(3,4,5)^2$12G2-CTV-3 to $(3,4,5)^2$dm8*G2-CTV-3 did not change the sequence of columnar structures of their supramolecular assemblies. In the cases of (4−3,4,5)12G1-CTV and (3,4−3,5)12G2-CTV the nonchiral dendritic crown exhibited both Φ_h^{io} and *Pm*$\bar{3}$*n* cubic structure. The incorporation of the branched stereocenter created (4−3,4,5)dm8*G1-CTV and (3,4−3,5)dm8*G2-CTV that eliminated the assembly in the Φ_h^{io} phase and maintained only the *Pm*$\bar{3}$*n* cubic phase (Table 1). In the case of $(3,4,5)^2$12G2-CTV-3 the incorporation of the sterecenter maintained the $P4_2/mnm$ tetragonal phase (Table 1). The analysis of all chiral cubic and tetragonal lattices is summarized in Tables 2 and 3. Figure 8 compares the supramolecular sphere self-assembled from the conical conformer of (3,4−3,5)dm8*G2-CTV with the supramolecular sphere assembled from a fragment of helical pyramidal column. As in the previous discussion on (4−3,4,5)12G1-CTV, the helical pyramidal model is preferred for the generation of a supramolecular sphere with diameter closed to that obtained by XRD experiments (Figure 8, Table 2).

An additional experiment that supports the hypothesis that short helical pyramidal columns form helical supramolecular spheres is shown in Figure 9. This figure illustrates the electron density map profile of the unit cell (Figure 9a) of the *Pm*$\bar{3}$*n* cubic lattice and of its $z = 0$ plane (Figure 9b). In Figure 9c, the electron density profiles reconstructed from XRD, the molecular models generated from the crown and conical models of assembly are compared as a function of *R*. The experimental electron density profile determined from XRD data agree much better with the crown-like model rather than the conical model.

The explanation for the elimination of the Φ_h^{io} phase by the introduction of the branched stereocenter and for the assembly of supramolecular sphere and the formation of the *Pm*$\bar{3}$*n* cubic phase is suggested by the dendritic crown conformation shown in Figure 10. The steric constrains present in the crowded aromatic region of the dendronized CTV core generate a minimum torsion angle. Furthermore, a direct correlation between the dendron solid angle, minimum torsion angle, and

Table 2. Structural and Retrostructural Analysis of the Dendronized CTV

dendrimer	T (°C)	phase	$d_{(200)}$[a] $d_{(10)}$[b] (Å)	$d_{(210)}$[a] $d_{(11)}$[b] (Å)	$d_{(211)}$[a] $d_{(20)}$[b] (Å)	A (Å)	D_{sphere}^{exp} D_{col}exp[c] (Å)	ρ[d] (g/cm^3)	$\mu_{(cell)}$[e]	μ[f]
(4−3,4,5)12G1-CTV	130	$Pm\bar{3}n$	43.8[a]	39.2[a]	35.8[a]	87.6	54.3	1.02	67.3	8.4
	100	Φ_h^{io}	38.5[b]	22.1[b]	19.2[b]	44.3	44.3			
(3,4,5)12G1-CTV	80	$Pm\bar{3}n$	36.6[a]	32.7[a]	29.8[a]	73.5	45.6	1.02	57.7	7.2
	65	Φ_h^{io}	35.6[b]	20.5[b]	17.8[b]	41.1	41.1			
(3,4−3,5)12G2-CTV	110	$Pm\bar{3}n$	41.2[a]	37.0[a]	33.7[a]	82.5	51.2	1.02	52.2	6.5
	25	Φ_h^{io}	41.1[b]	23.7[b]	20.5[b]	47.4	47.4			
(4−3,4,5)dm8*G1-CTV	100	$Pm\bar{3}n$	40.3[a]	36.1[a]	32.9[a]	80.6	50.0	1.03	57.7	7.2
(3,4,5)dm8*G1-CTV	5	$Pm\bar{3}n$	31.1[a]	27.8[a]	25.4[a]	62.2	38.6	1.03	40.1	5.0
(3,4−3,5)dm8*G2-CTV	80	$Pm\bar{3}n$	37.4[a]	33.4[a]	30.5[a]	74.7	46.4	1.03	43.6	5.4

[a] d-spacings of the $Pm\bar{3}n$ cubic phase, their ratio is $\sqrt{4}:\sqrt{5}:\sqrt{6}$ and $a = (\sqrt{4}d_{200} + \sqrt{5}d_{210} + \sqrt{6}d_{211})/3$. [b] d-spacing of the Φ_h^{io} columnar hexagonal phase with intracolumnar order, their ratio is $1:\sqrt{3}:\sqrt{4}$ and $a = (2/\sqrt{3})(d_{10} + \sqrt{3}d_{11} + 2d_{20})/3$. [c] For $Pm\bar{3}n$ cubic phase spherical cluster diameter calculated using $D_{sphere} = 2a/(32\pi/3)^{1/3}$ and for columnar hexagonal phases column diameter calculated using $D_{col} = a$. [d] Experimental density measured at 20 °C. [e] Number of dendrimers in the $Pm\bar{3}n$ unit cell calculated using $\mu_{cell} = \rho a^3 N_A/M_{wt}$. [f] Number of dendrimers per supramolecular sphere calculated using $\mu = \mu_{cell}/8$.

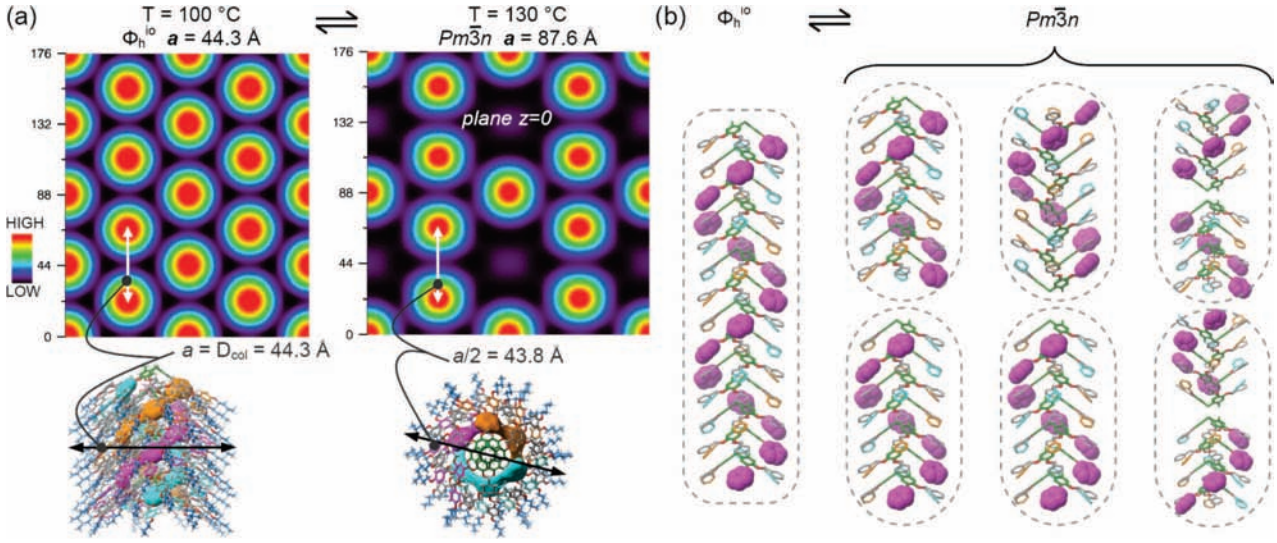

Figure 5. Reconstructed electron density maps (a) and the molecular models of (4−3,4,5)12G1-CTV that self-assemble into supramolecular helical columns at low temperatures and supramolecular spheres at high temperatures (b). In (a), the lattice dimensions and column or sphere diameters are indicated. In (b), the supramolecular columns or spheres are indicated by the dotted lines.

Table 3. Structural and Retrostructural Analysis of the Tri-substituted Dendronized CTV

dendrimer	T (°C)	phase	a, c[a] (Å)	$d_{(002)}$[b] $d_{(10)}$[c] (Å)	$d_{(410)}$[b] $d_{(11)}$[c] (Å)	$d_{(411)}$[b] $d_{(20)}$[c] (Å)	$d_{(312)}$[b] (Å)	D_{sphere}^{exp} D_{col}exp[d] (Å)	μ[e]
(3,4,5)^{2}12G2-CTV-3	90	$P4_2/mnm$	145.4, 76.9	38.5[b]	35.2[b]	32.1[b]	29.5[b]	41.2	5.0
(3,4,5)^{2}dm8*G2-CTV-3	70	$P4_2/mnm$	140.5, 73.3	36.6[b]	34.1[b]	30.9[b]	28.3[b]	39.7	5.0
(4−3,4−3,5)12G2-CTV-3	130	Φ_h^{io}	44.5, -	38.5[c]	22.3[c]	19.3[c]		44.5	
(4−3,4−3,5)dm8*G2-CTV-3	35	Φ_h^{io}	41.4, -	35.9[c]	20.7[c]	17.9[c]		41.4	

[a] Lattice parameters $a = b$, c for the $P4_2/mnm$ tetragonal phase and a for the Φ_h^{io} columnar hexagonal phase with intracolumnar order. [b] d-spacing of the $P4_2/mnm$ tetragonal phase. [c] d-spacing of the Φ_h^{io} columnar hexagonal phase with intracolumnar order, their ratio is $1:\sqrt{3}:\sqrt{4}$ and $a = (2/\sqrt{3})(d_{10} + \sqrt{3}d_{11} + 2d_{20})/3$ [d] Column or sphere diameter calculated using $D_{sphere} = a\sqrt{2}/5$ for the $P4_2/mnm$ tetragonal phase and $D = a$ for the Φ_h^{io} phase. [e] Number of dendrimers per supramolecular sphere calculated for the $P4_2/mnm$ tetragonal phase using $\mu_{sphere} = \rho a^2 c N_A/(30M_{wt})$, where N_A = Avogadro's number, $\rho = 1.0$ g/cm^3 density, and M_{wt}- molecular weight.

the formation of cubic phases is illustrated in Figure 10. Dendrons with large solid angle require a larger tosion angle than those with smaller solid angle and, therefore, are more likely to self-assemble into supramolecular spheres.

Analysis of Chiral Supramolecular Spheres Assembled from Chiral Dendritic Crowns by CD Experiments. CD experiments were carried out in solvophobic solvents and on thin films. Both solution and thin film experiments were tested for possible artifacts derived from linear dichroism.[17] The preparation of the thin films for these experiments and the demonstration of the absence of linear dichroism are described in the Supporting Information. An experiment that demonstrates that the supramolecular structures assembled in bulk state and in solution are similar is shown in Figure 11. The assembly of (3,4)dm8*G1-CTV that was shown previously[13] to form a helical pyramidal column was monitored by CD experiments in the solvophobic solvent dodecane and in thin film cast from $CHCl_3$. With the exception of the ellipticity and temperature range both CD spectra show a remarkable similarity. In both cases, isodichroic points that support an equilibrium between the molecular dendritic crown and its helical pyramidal supramolecular column

(17) (a) Saeva, F. D.; Olin, G. R. *J. Am. Chem. Soc.* **1977**, *99*, 4848–4850. (b) Palmans, A. R. A.; Meijer, E. W. *Angew. Chem., Int. Ed.* **2007**, *46*, 8948–8968. (c) Wolffs, M.; George, S. J.; Tomovic, Z.; Meskers, S. C. J.; Schenning, A. P. H. J.; Meijer, E. W. *Angew. Chem., Int. Ed.* **2007**, *46*, 8203–8205. (d) Tsuda, A.; Alam, M. A.; Harada, T.; Yamaguchi, T.; Ishii, N.; Aida, T. *Angew. Chem., Int. Ed.* **2007**, *46*, 8198–8202.

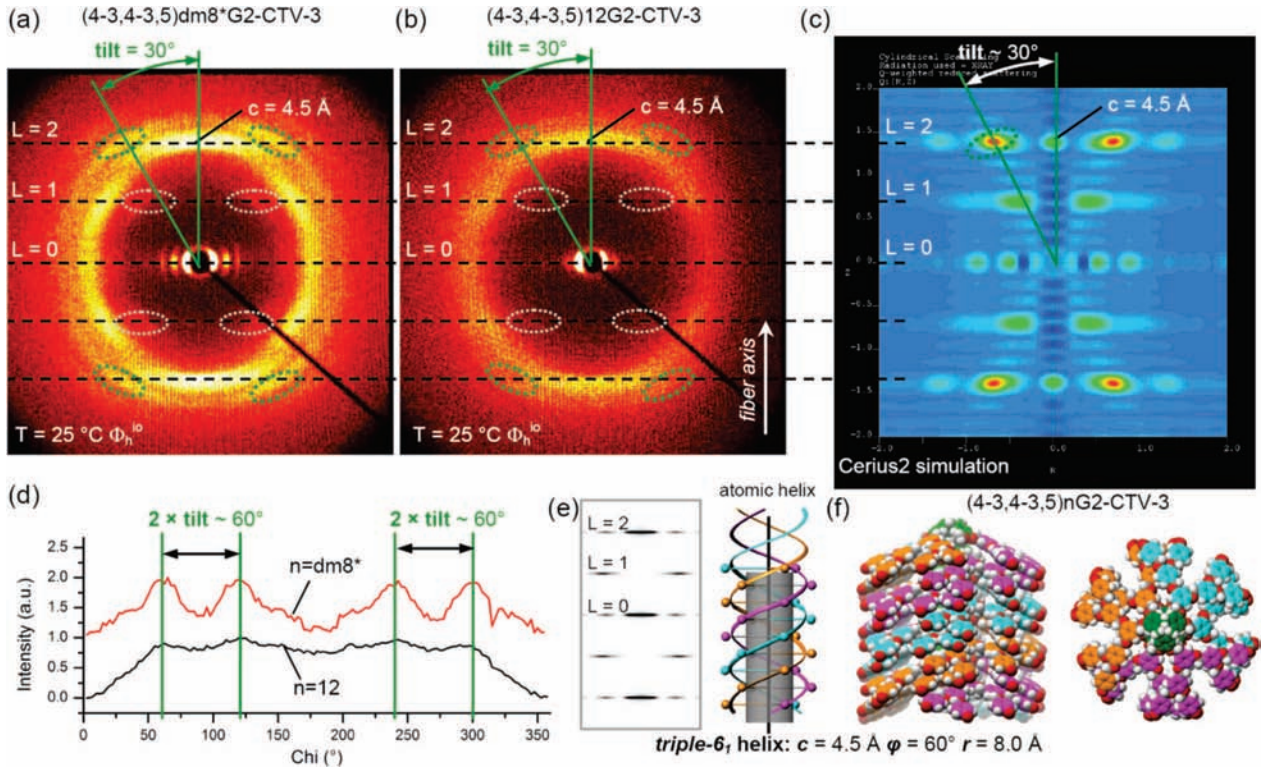

Figure 6. Wide-angle oriented fiber XRD patterns collected from the Φ_h^{io} lattices of the chiral (4−3,4−3,5)dm8*G2-CTV-3 (a) and achiral (4−3,4−3,5)12G2-CTV-3 (b). The molecular model based Cerius2 simulation of the oriented fiber XRD patterns (c). The azimuthal angle Chi plots vs intensity integrating the q-range around the dendron tilt features marked by green dotted circles in a and b (d). The identified atomic helix, the corresponding helical fiber pattern simulation, and the triple helix parameters (e). Side and top space filling views of the molecular model used in the Cerius2 simulation (f).

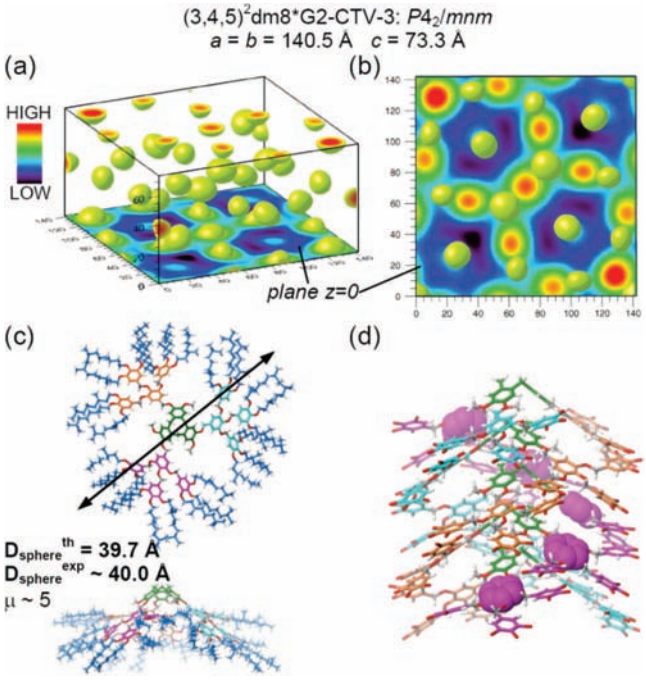

Figure 7. The reconstructed electron density of the $P4_2/mnm$ unit cell of $(3,4,5)^2$dm8*G2-CTV-3 (a, b), the corresponding molecular model (c), and detail of the aromatic core packing (d). In (a), only the regions with high electron density and the plane $z = 0$ are shown. Color code in (c) and (d): each dendron aromatic region is orange, light blue and magenta, respectively; CTV, green; alkyl chains C atoms, dark blue; O atoms, red; H atoms, white; and all the other C atoms, gray.

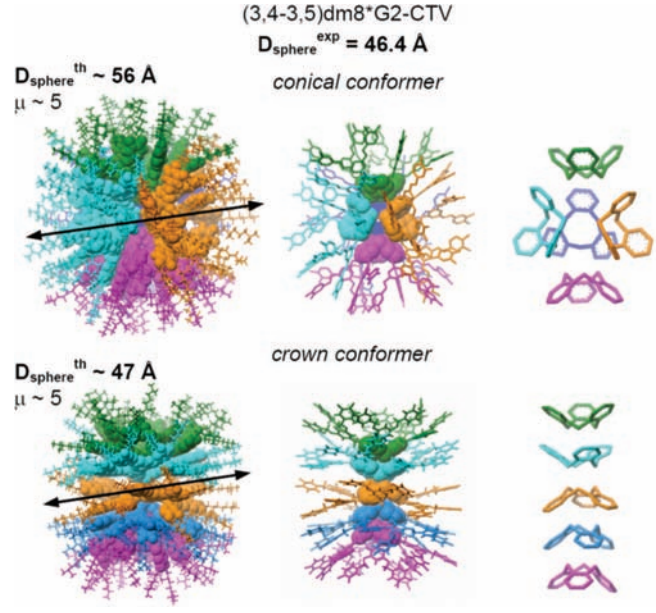

Figure 8. Molecular models of the spherical supramolecular dendrimer assembled from (3,4−3,5)dm8*G2-CTV by the conical and crown conformer models. From left to right: supramolecular sphere, detail of the aromatic region, and the CTV core region.

are observed. They are supported by isosbestic points seen in the corresponding UV spectra (Figure SF1 in Supporting Information). As expected, the major difference between film and solution consists of a higher stability of the helical pyramidal column observed in bulk state. On the basis of this analysis, it is expected that the arrangement of the dendritic crown in the supramolecular sphere consists of a helical pyramidal column similar but shorter than the one observed in the Φ_h^{io} phase. An additional CD experiment for the newly synthesized (4−3,4−

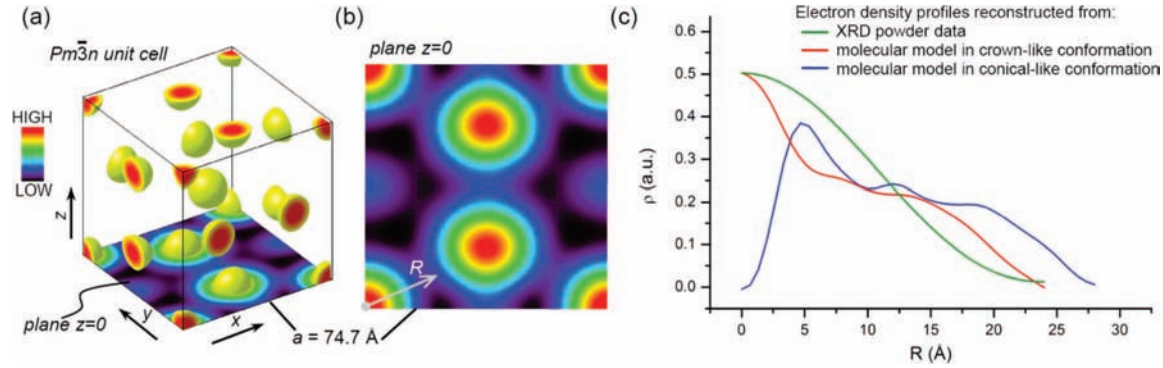

Figure 9. Relative electron density distribution within the unit cell of the $Pm\bar{3}n$ lattice of (3,4−3,5)dm8*G2-CTV (a). Electron density in $z = 0$ plane (b). Relative electron densities within each supramolecular sphere calculated from the XRD powder data (green curve), molecular model of the crown-like conformation (red curve), and molecular model of the conical-like conformation (blue curve) (c). The electron densities were extracted from the molecular model using Gaussian functions.

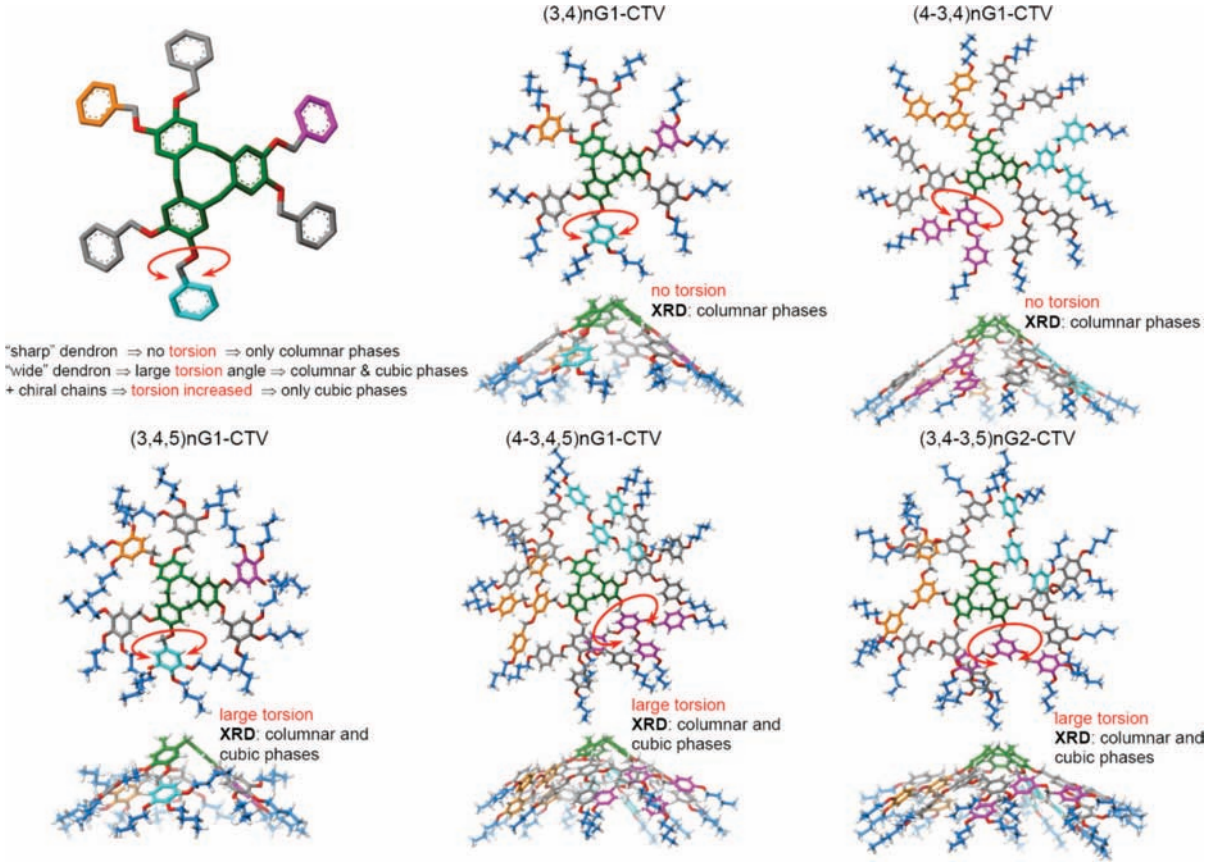

Figure 10. Molecular models of the dendronized CTV crowns. The direct correlation between the presence of a cubic phase and dendron architecture is illustrated by the marked torsion angle required to fit the conformer in the supramolecular structure determined by XRD.

3,5)dm8*G2-CTV-3 is in line with the helical pyramidal columnar structure (Figure 6, Table 3).

The temperature and concentration dependence of the CD spectra in solution and film of all the chiral dendritic crowns that self-assemble in spherical supramolecular dendrimers and self-organize in $Pm\bar{3}n$ cubic or $P4_2/mnm$ tetragonal lattices resemble the behavior of those shown in Figure 11. Figure 12 summarizes selected examples of CD spectra compared in film and in solution. Figure 12, parts a and b, compares CD spectra of the spherical supramolecular assembly generated by the chiral dendritic crown (3,4,5)dm8*G1-CTV in film and in dodecane. An expansion of the spectra from Figure 12b is provided in Figure SF2 (Supporting Information). As in the case of the results from Figure 11 obtained for helical pyramidal columns from (3,4)dm8*G1-CTV the spherical supramolecular spheres assembled from (3,4,5)dm8*G1-CTV exhibit a lower arbitrary ellipticity in thin film than in solution and a lower stability in solution. The CD spectra in solution and film obtained for the spherical supramolecular assemblies generated from (3,4−3,5)dm8*G2-CTV are shown in Figure 12c,d. These supramolecular spheres as the one from Figure 12a,b self-organize in a $Pm\bar{3}n$ cubic lattice. A similar CD trend is observed. The CD spectra from Figure 12, parts e and f are representative for the assembly of $(3,4,5)^2$dm8*G2-CTV-3 into spherical assemblies that self-organize $P4_2/mnm$ tetragonal lattice. UV spectra for all CD data for Figure 12 are available in Supporting Information (Figure SF2).

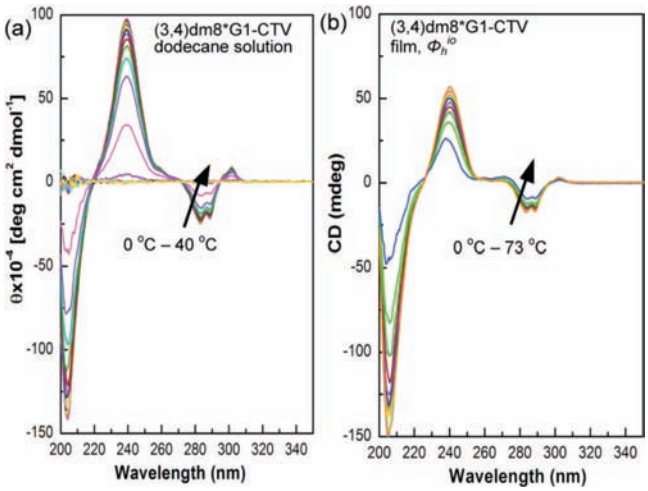

Figure 11. Temperature dependence of the CD spectra of (3,4)dm8*G1-CTV in dodecane solution (6.0×10^{-5} M) (a) and in spin-coated film cast from $CHCl_3$ (1.8%, w/v) (b). Arrows indicate trends upon increasing temperature.

The brief CD analysis reported in Figure 12 demonstrates that the supramolecular spheres assembled from chiral dendritic crown are chiral and that this chirality is produced by the internal structure of the supramolecular sphere. All XRD and CD data reported here support a new mechanism for the assembly of dendritic crowns in spherical supramolecular dendrimers that involves short helical pyramidal columns (see μ in Tables 2 and 3). These short helical pyramidal columns explain the lower ellipticity of the CD spectra of the chiral supramolecular spheres when compared with the CD spectra of the helical pyramidal columns.

Mechanism of Chiral Induction in a Spherical Supramolecular Dendrimer. As mathematically described, a sphere cannot be chiral. However, there are several examples of objects with approximately spherical shape that are chiral. For example, there are chiral colloidal clusters aggregated from spherical colloids.[18] Gold nanoparticles exhibiting chirality have also been reported although the origin of their chirality is still debated.[19a−d] Several mechanisms were advanced for the origin of chirality in gold nanoparticles: (a) the interior of the particle is chiral; (b) the thiol groups on the gold surface generate a chiral pattern;

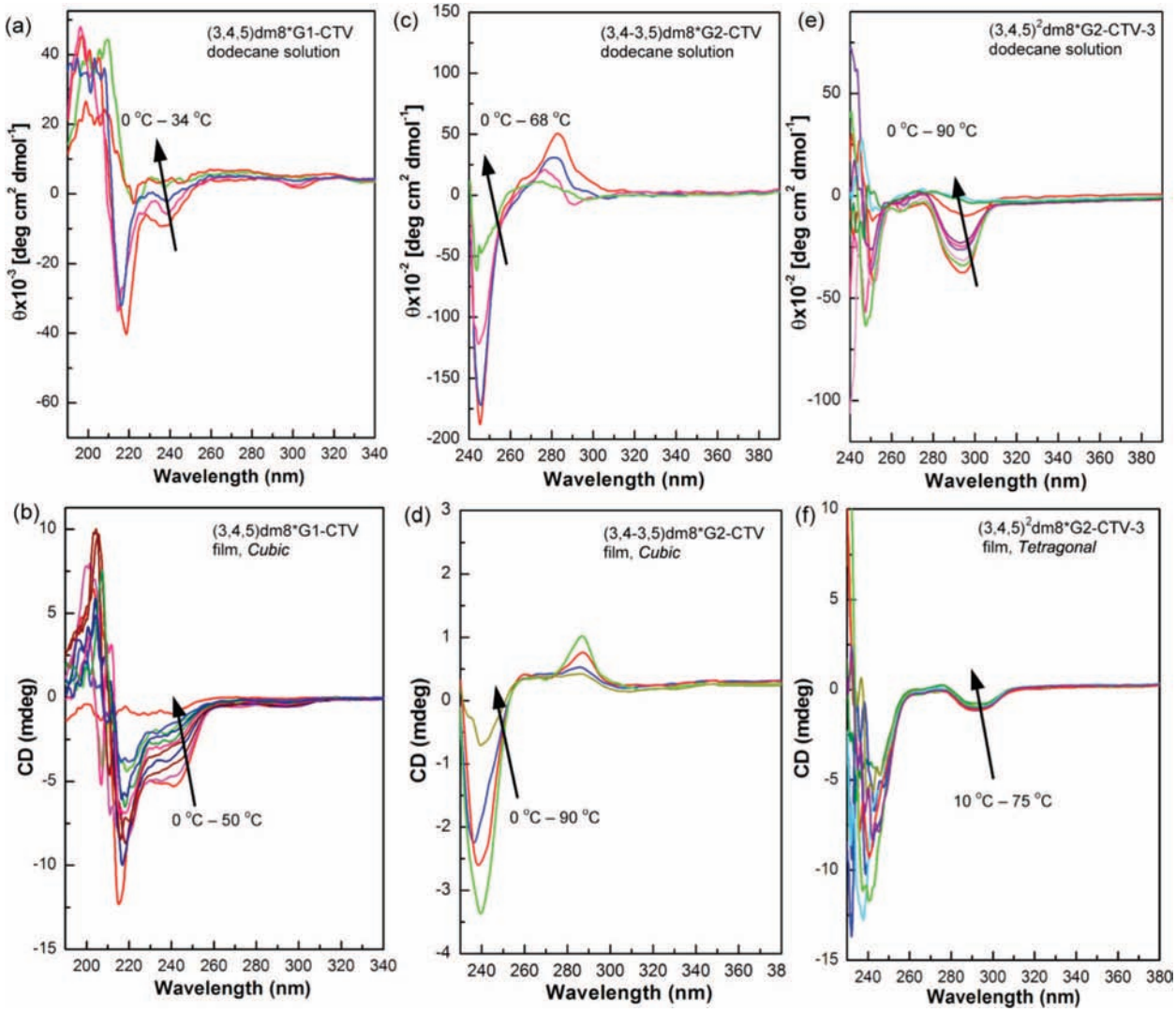

Figure 12. Temperature dependence of the CD spectra of (3,4,5)dm8*G1-CTV in dodecane solution (6.0×10^{-5} M) (a) and in spin-coated film of the cubic structure cast from $CHCl_3$ (2.5% w/v) (b); of (3,4−3,5)dm8*G2-CTV in dodecane solution (2.4×10^{-4} M) (c) and in spin-coated film of the cubic structure cast from $CHCl_3$ (4.5%, w/v) (d); of $(3,4,5)^2$dm8*G2-CTV-3 in dodecane solution (8.3×10^{-4} M) (e) and in spin-coated film of the tetragonal structure cast from $CHCl_3$ (6.4% (w/v) (f). Arrows indicate trends upon increasing temperature.

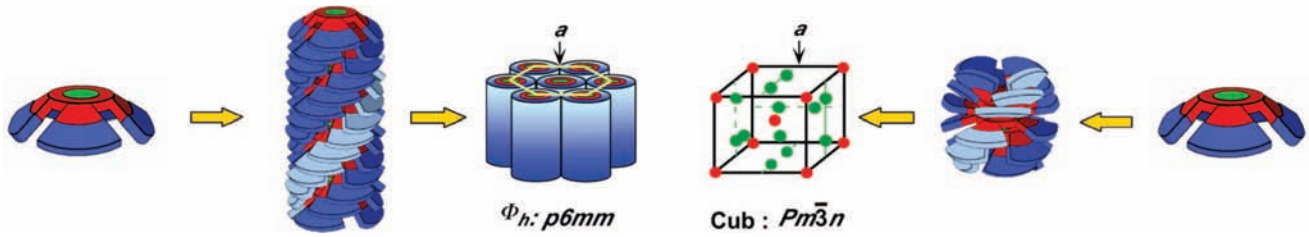

Figure 13. The new mechanism of self-assembly of spherical supramolecular dendrimers involving helical pyramidal columns.

(c) the gold nanoparticle exhibits a chiral polygonal shape.[19a−d] Internal helical spherical contours known as a helical sphere, loxodrome, or rhumb[20] were previously suggested to be responsible for the chirality of spherical supramolecular dendrimers exhibiting a helical cage.[11] Molecular apple peels are other examples of spherical chiral capsules.[21] An example of a dendronized folic acid that exhibited chirality in a $Pm\bar{3}n$ cubic phase upon complexation with $NaOSO_2CF_3$ was also reported.[19e] A helical discotic-like internal arrangement was suggested for its optical activity although no wide-angle XRD experiments were reported in its Φ_h phase to confirm the suggested structure. The supamolecular dendrimers reported here are approximately spherical in shape. But, of course, being made of atoms, they are not indeed mathematical spheres. The results reported here demonstrate that an internal pyramidal column is responsible for the chirality exhibited by these spherical supramolecular dendrimers. The most probable mechanism of assembly is illustrated in Figure 13. The inversion of the CTV crown in isotropic solution or melt state is fast. However, its rotation barrier decreases in an ordered state.[14e] Therefore, discrimination between the models of helical pyramidal structures responsible for the generation of the chiral spheres shown in Figure 5b is not possible without additional experiments involving more advanced NMR and XRD methods. Most probably, even the supramolecular spherical dendrimers generated from nonchiral dendrons are chiral but do not exhibit a CD spectrum since these are racemic. Therefore, we suggest that the role of the stereocenter is simply to select the handedness of an already helical structure.[12,22] Conventional self-assembling dendrons and dendrimers have been shown to exhibit crown conformations[12] and therefore, the self-assembly mechanism reported here is expected to be encountered in many other classes of self-assembling dendrons and dendrimers. The cavity of CTV acts as a host to many examples of gusts[9f−j] and therefore, spherical supramolecular dendrimers that exhibit chirality are expected to exhibit host−guest interactions. The transfer of chirality by the helical pyramidal architecture available both in Φ_h^{io} and $Pm\bar{3}n$ phases is also expected to provide new information on the mechanism of transfer of structural information. The development of new supramolecular concepts generated by the self-assembly mechanism elaborated here is under investigation.

Conclusions

The synthesis, structural, and retrostructural analysis of a library containing fourteen dendronized CTV is reported. Seven of these dendronized CTV are chiral and seven are nonchiral. All dendronized CTV exhibit a crown conformation that we call dendritic crown. Dendritic crowns self-assemble in helical pyramidal columns and spherical supramolecular dendrimers that are chiral. Both the helical pyramidal columns and the supramolecular spheres generated from nonchiral dendrons are chiral but racemic while those generated from chiral dendrons amplify their molecular chirality[17b] in solution and in bulk and are chiral. A combination of X-ray diffraction methods and CD experiments were used to demonstrate that the internal structure of the spherical supramolecular dendrimers generated from dendritic crowns consists of short fragments of helical pyramidal columns. This new self-assembly process is expected to provide access to new mechanisms[17b] for the transfer and amplification of structural information from the molecular to supramolecular level, to clarify concepts related to the chirality of dendritic macromolecules,[23] and to generate new fundamental and technological concepts mediated by chiral supramolecular dendrimers.

Acknowledgment. Financial support by the National Science Foundation (DMR-0548559 and DMR-0520020) and the P. Roy Vagelos Chair at Penn is gratefully acknowledged. We thank Professor G. Ungar from the University of Sheffield, UK for helpful discussions.

Supporting Information Available: Experimental synthetic procedures with complete spectral, structural and retrostructural analysis (PDF). This material is available free of charge via the Internet at http://pubs.acs.org.

JA8087778

(18) (a) Pickett, G. T.; Gross, M; Okayama, H. *Phys. Rev. Lett.* **2000**, *85*, 3652–3655. (b) Yin, Y.; Xia, Y. *J. Am. Chem. Soc.* **2003**, *125*, 2048–2049. (c) Snir, Y.; Kamien, R. D. *Science* **2005**, *307*, 1067. (d) Zerrouki, D.; Baudry, J.; Pine, D.; Chaikin, P.; Bibette, J. *Nature* **2008**, *455*, 380–382.

(19) (a) Qi, H.; Hegmann, T. *J. Am. Chem. Soc.* **2008**, *130*, 14201–14206. (b) Schaaff, T. G.; Whetten, R. L. *J. Phys. Chem. B* **2000**, *104*, 2630–2641. (c) Gautier, C.; Bürgi, T. *J. Am. Chem. Soc.* **2008**, *128*, 11079–11087. (d) Jadzinsky, P. D.; Calero, G.; Ackerson, C. J.; Bushnell, D. A.; Kornberg, R. D. *Science* **2007**, *318*, 430–433. (e) Kato, T.; Matsuoka, T.; Nishii, M.; Kamikawa, Y.; Kanie, K.; Nishimura, T.; Yashima, E.; Ujiie, S. *Angew. Chem., Int. Ed.* **2004**, *43*, 1969–1972.

(20) (a) Alexander, J. *Math. Mag.* **2004**, *77*, 349–356. (b) Thompson, D. A. W. *On Growth and Form; Cambridge University Press* **1961**, *172*, p 201.

(21) (a) Garric, J.; Léger, J.-M.; Huc, I. *Angew. Chem., Int. Ed.* **2005**, *44*, 1954–1958. (b) Garric, J.; Léger, J.-M.; Huc, I. *Chem. -Eur. J.* **2007**, *13*, 8454–8462. (c) Bao, C.; Kauffmann, B.; Gan, Q.; Srinivas, K.; Jiang, H.; Huc, I. *Angew. Chem., Int. Ed.* **2008**, *47*, 4153–4156.

(22) (a) Green, M. M.; Park, J.-W.; Sato, T.; Teramoto, A.; Lifson, S.; Selinger, R. L. B.; Selinger, J. V. *Angew. Chem., Int. Ed.* **1999**, *38*, 3138–3154. (b) Jonkheijm, P.; van der Schoot, P.; Schenning, A. P. H. J.; Meijer, E. W. *Science* **2006**, *313*, 80–83. (c) Percec, V.; Ungar, G.; Peterca, M. *Science* **2006**, *313*, 55–56. (d) Yashima, E.; Maeda, K.; Furusho, Y. *Acc. Chem. Res.* **2008**, *41*, 1166–1180. (e) Katsonis, N.; Xu, H; Haak, R. M.; Kudernac, T.; Tomovic, Z.; George, S.; Van der Auweraer, M.; Schenning, A. P. H. J.; Meijer, E. W.; Feringa, B. L.; De Feyter, S. *Angew. Chem., Int. Ed.* **2008**, *47*, 4997–5001. (f) Jin, W.; Fukushima, T.; Niki, M.; Kosaka, A.; Ishii, N.; Aida, T.; Noyori, R. *Proc. Natl. Acad. Sci. U. S. A.* **2005**, *102*, 10801–10806. (g) van Gestel, J.; Palmans, A. R. A.; Titulaer, B.; Vekemans, J. A. J. M.; Meijer, E. W *J. Am. Chem. Soc.* **2005**, *127*, 5490–5494.

(23) (a) Seebach, D.; Rheiner, P. B.; Greiveldinger, G.; Butz, T.; Sellner, H. *Top. Curr. Chem.* **1998**, *197*, 125–164. (b) Peerlings, H. W. I.; Meijer, E. W. *Chem. -Eur. J.* **1997**, *3*, 1563–1570. (c) Thomas, C. W.; Tor, Y. *Chirality* **1998**, *10*, 53–59.